Biosensors and Bioelectronics 107 (2018) 1–9

Contents lists available at ScienceDirect

Biosensors and Bioelectronics

journal homepage: www.elsevier.com/locate/bios

# A disposable immunosensor using ITO based electrode modified by a star-shaped polymer for analysis of tumor suppressor protein p53 in human serum

Muhammet Aydın[a], Elif Burcu Aydın[a,*], Mustafa Kemal Sezgintürk[b]

[a] Namık Kemal University, Scientific and Technological Research Center, Tekirdağ, Turkey
[b] Çanakkale Onsekiz Mart University, Faculty of Engineering, Bioengineering Department, Çanakkale, Turkey

ARTICLE INFO

*Keywords:*
Protein p53
Electrochemical impedance spectroscopy
Cyclic voltammetry
Single frequency impedance
Star-polymer
Poly(glycidyl methacrylate)

ABSTRACT

Label-free immunosensor based on tetra armed star-shaped poly(glycidylmethacrylate) (**Star$_{PGMA}$**) modified disposable ITO electrode was developed for detection of p53 protein, an important colorectal cancer biomarker. This disposable biosensor was fabricated by spin-coating technique using star-shaped **Star$_{PGMA}$** with epoxy side groups. After formation of a stable film with epoxy ends, anti-p53 antibodies were bound to these groups covalently. Stepwise modification of the electrode was followed by electrochemical impedance spectroscopy (EIS) and cyclic voltammetry (CV) studies. The electrochemical performance of the immunosensor was studied by EIS. Furthermore, the antibody and antigen coupling was monitored by single frequency impedance (SFI) technique. The immunosensor showed a low limit of detection (7 fg/mL) and a linear detection range between 0.02 pg/mL and 4 pg/mL. Additionally, atomic force microscopy (AFM) and scanning electron microscopy (SEM) were utilized for monitoring of immunosensor surface at different stages of fabrication. The antibody coupling on the electrode surface was proved by Fourier-transform infrared spectroscopy (FTIR) and Raman spectroscopy. Furthermore, the proposed immunosensor had good reproducibility and repeatability.

## 1. Introduction

Early stage cancer diagnosis by monitoring cancer biomarkers in human biological fluids has received attention in recent years (Feng et al., 2006). Cancer threats human health and colorectal cancer causes cancer-related deaths in the world. Furthermore, it is the third deadliest of all cancers. In colorectal cancer, the abnormal growth occurs in the colon and rectum. The abnormal growth causes formation of a tumor on the wall of the rectum or colon, and then grows into blood vessels or lymph vessels, and other anatomical sites (Marley and Nan, 2016). If detected early, before metastasis has occurred, the chance of survival following surgical resection of the tumor is > 90%. Early detection is therefore critical for effective disease surveillance. However, current biomarker assays lack the necessary sensitivity and specificity for reliable early disease detection. Development of new robust, non-or minimally invasive specific and sensitive biomarkers or panels with improved performance is required (Fung et al., 2015).

Protein p53 is a significant biomarker in tumor suppressing process and has an important role in cellular functions such as cell growth and proliferation, DNA repair, and apoptosis (Afsharan et al., 2016a). Loss of p53 function causes the induction of tumors and gene mutation, therefore a conformational change is formed in the structure of p53 protein (Chen et al., 2012). During mutation, the cell proliferation is formed and it results in tumor formation. After destruction of tumor cells, p53 protein is released from cancer cells and penetrates into the circulation (Afsharan et al., 2016b). The level of p53 protein is ranged from 0.52 ± 0.23 ng/mL to 1.03 ± 0.59 ng/mL in serum samples from cancer patients (Attallah et al., 2003). An important increase in the serum level is a sign of different types of cancers like colorectal. The accurate and sensitive detection of p53 protein is important due to these significant roles of p53. Nowadays, a lot of techniques have been utilized for p53 protein detection. These techniques include enzyme-linked immunosorbent assay (ELISA), high performance liquid chromatography (HPLC), surface plasmon resonance, surface enhanced Raman spectroscopy, immunohistochemical method (Afsharan et al., 2016a), Western blotting (Bryś et al., 2000). Methods based on chromatography have been rarely utilized for p53 detection. Ben-Hur et al. (1997) used HPLC to measure serum levels of p53 protein with a gel fiberglass affinity chromatography column. Zusman (1998) used a gel fiberglass membranes for affinity chromatography column for the isolation of p53 protein from the serum of cancer patients. For the detection of a biomarker, ELISA method is usually utilized. Although

* Corresponding author.
*E-mail addresses:* b_e_bahadir@hotmail.com, ebbahadir@nku.edu.tr (E.B. Aydın).

https://doi.org/10.1016/j.bios.2018.02.017
Received 27 October 2017; Received in revised form 5 January 2018; Accepted 4 February 2018
Available online 05 February 2018
0956-5663/ 

ELISA is a successful technique for the determination of p53 antigens, this technique requires a lot of time to perform the analysis procedure and also expensive devices. Furthermore, a variety of commercial kits are available. Attallah et al. (2003) used ELISA kit for p53 protein detection in serum. Furthermore, they used Western blotting as a gold standard for ELISA. They found 91% agreement between the results of Western blotting and ELISA for 55 serum samples of cancer patients. Biosensors are fascinating tools for rapid, sensitive and low-cost detection of several analytes (Turner, 2013). Therefore, they have gained interest in the past few decades. When ELISA technique is compared to electrochemical immunosensors, they are more specific, sensitive, reliable, rapid and lower cost. Electrochemical immunosensors with different modification strategies have drawn a lot of attention in recent years and are utilized for the determination of p53 antigens (Wang et al., 2015). Some of these biosensors are summarized in SI-Table 1. Chen et al. developed a magnetic particle based immunosensor for phosphorylated p53 protein detection. To increase the sensitivity of the biosensor carbon nanospheres and protein cage nanoparticles were used for signal amplification. They found limit of detection (LOD) value as 10 fg/mL (Chen et al., 2012). In another study, Wang et al. (2015) fabricated an enzyme electro-catalytic biosensor based on carboxylated multi walled carbon nanotube (MWCNT) doped nylon 6 composite nanofiber modified glassy carbon electrode. This nanocomposite was modified on working electrode after poly(thionine) polymerization. These materials promoted electron transfer and provided a large surface area. This biosensor had wide linear detection range (2 pg/mL-2 ng/mL) and low detection limit (1 pg/mL) (Wang et al., 2015).

Electrochemical impedance spectroscopy (EIS) is a label-free and successful method, which has been utilized in the determination of a number of biomarkers (Bahadır and Sezgintürk, 2015; Topkaya et al., 2016; Wang et al., 2017a; Karimi-Maleh et al., 2013). By using this method, the variations in capacitance or charge-transfer resistance originated from the specific binding of biorecognition elements to their desired molecules, which formed on the electrode surface can be monitored. Therefore, it has been successfully utilized for the detection of several molecules (Bahadır and Sezgintürk, 2016c; Xu et al., 2013). Single frequency impedance (SFI) technique is used to follow changes in electrochemical impedance versus time. In this technique, electrochemical impedance is measured at one frequency periodically (Aydın et al., 2017; Aydın and Sezgintürk, 2017). In this study, we used SFI technique to follow antibody and antigen interactions.

The main step of the biosensor fabrication is the construction of immobilization matrix for biosensing element. Immobilization matrix is important to obtain stable and long-life biosensor and it should fix the biosensing element on the electrode surface and protect the structure of the biosensing element during the experiments (Soylemez et al., 2015). For this purpose, different types of polymers such as polyaniline, polythiophene have been used in biosensing applications (Ruecha et al., 2014). Star-shaped polymers are the best candidate for production of convenient matrix for biorecognition molecule immobilization. Star polymers are branched macromolecules and have several same or different linear polymer chains that attached to only one branching point (Inoue, 2000). Star-shaped polymers have several advantages such as higher solubilities, globular shape, lower solution and less chain entanglements than linear analogues with the same molecular weight. Star polymers resemble dendrimer from many aspects such as having a lot of active end groups. The advantage of using star polymers instead of dendrimer is their low cost (Gao and Matyjaszewski, 2009). Although there are a lot of biosensors based on dendrimer as immobilization matrix in literature, the scientific papers reporting star-shaped polymers as immobilization matrix are very rare (Bahadır and Sezgintürk, 2016b; Satija et al., 2011). For instance, Makelane et al. (2015) synthesized a dendritic star-copolymer for phenanthrene sensing. However, studies based on star polymer modified immunosensors were not found in literature. Therefore, this study will open the door in combination of star polymer and biosensor technology.

Spin coating is a simple technique to form uniform thin films on flat substrates. The principle of this method is based on the deposition of a small drop of a fluid onto the center of a material and then spinning of the material at high speed (Jeon et al., 2014). Centrifugal force will provide spreading the fluid and forming a thin film of fluid onto substrate surface (Tyona, 2013). Spin-coating is usually used for reproducible production of uniform thin film coatings on different areas. This technique is utilized in several applications such as coating of photoresist on silicon wafers, sensors, protective coatings, paint coatings, optical coatings and membranes. In sensor application, this technique focuses on spin-coating of polymer films on the sensor surfaces (Norrman et al., 2005). El-Said and Choi (2014) and El-Said and Choi (2014) formed a polystyrene (PS) film and Singh et al. (2016) formed a thin film of graphene oxide on the ITO electrode.

In this study, we aimed the development of a star polymer based immunosensor with antibodies as biorecognition element to detect p53 antigen with high specificity. We used star-shaped (**Star$_{PGMA}$**) as immobilization matrix for immobilization of anti-p53 antibodies. For this purpose, an initiator compound containing four bromide functional groups was prepared through a facile esterification reaction. A tetra-armed polymer **Star$_{PGMA}$** with glycidyl side groups was synthesized by using atom transfer radical polymerization (ATRP) in the presence of tetra functional initiator. Then, polymer **Star$_{PGMA}$** formed a film on the ITO electrode by using spin coating technique. Anti-p53 antibodies bound to epoxy group of **Star$_{PGMA}$** covalently. The covalent coupling of antibodies on the ITO electrode surface was proved by using FTIR and RAMAN spectral techniques. Electrochemical and morphological characterizations of electrode modification steps were performed by EIS and CV, and AFM and SEM, respectively. To evaluate high sensitivity and wide detection range, experimental conditions were optimized. Furthermore, the specific interaction between antibody and antigen was monitored by SFI technique. To investigate clinically applicability, real human samples were analyzed by using this immunosensor and in order to prove accuracy of the method, standard addition technique was utilized. The proposed biosensor shows great promise for the early clinical diagnosis of p53 antigens.

## 2. Materials and methods

### 2.1. Materials

The inhibitors of glycidyl methacrylate (GMA, Sigma-Aldrich, 97%) was removed by running through from basic alumina column and was freshly used. Pentaerythritol (Sigma-Aldrich, 99%), N,N,N′,N″,N″-Pentamethyldiethylenetriamine (PMDETA, Sigma-Aldrich, 99%), Copper(I) bromide (Sigma-Aldrich, 98%), α-Bromoisobutyryl bromide (Sigma-Aldrich, 98%), and anisole (anhydrous, Sigma-Aldrich, 99.7%) were used without further purification. Triethylamine (TEA, Sigma-Aldrich, ≥ 99%) was distilled over potassium hydroxide before use. Indium tin oxide (ITO) electrodes (5 mm × 20 mm, 60 Ω/cm$^2$), monoclonal anti-p53 antibody, p53 human recombinant antigen were obtained from Sigma-Aldrich. Anti-p53 antibody, recombinant human p53 and bovine serum albumin (BSA) solutions were prepared using phosphate buffer (PBS 50 mM, pH 7.0) and stored at − 20 °C. Ferri-ferro solution contained 1 M KCl, 5 mM $[Fe(CN)_6]^{-4}$ and 5 mM $[Fe(CN)_6]^{-3}$ in PBS and was utilized as redox probe.

### 2.2. Instrumentation

All electrochemical experiments were carried out in a conventional three-electrode cell containing a disposable ITO electrode, a platinum wire and Ag/AgCl as a working electrode, a counter electrode and a reference electrode, respectively. Electrochemical studies were carried out in the presence of $[Fe(CN)_6]^{3-/4-}$ as redox couple and a Gamry Potentiostat/Galvanostat (Reference 1000, Gamry Instruments, Warminster, PA, USA) was used for EIS and CV measurements. The

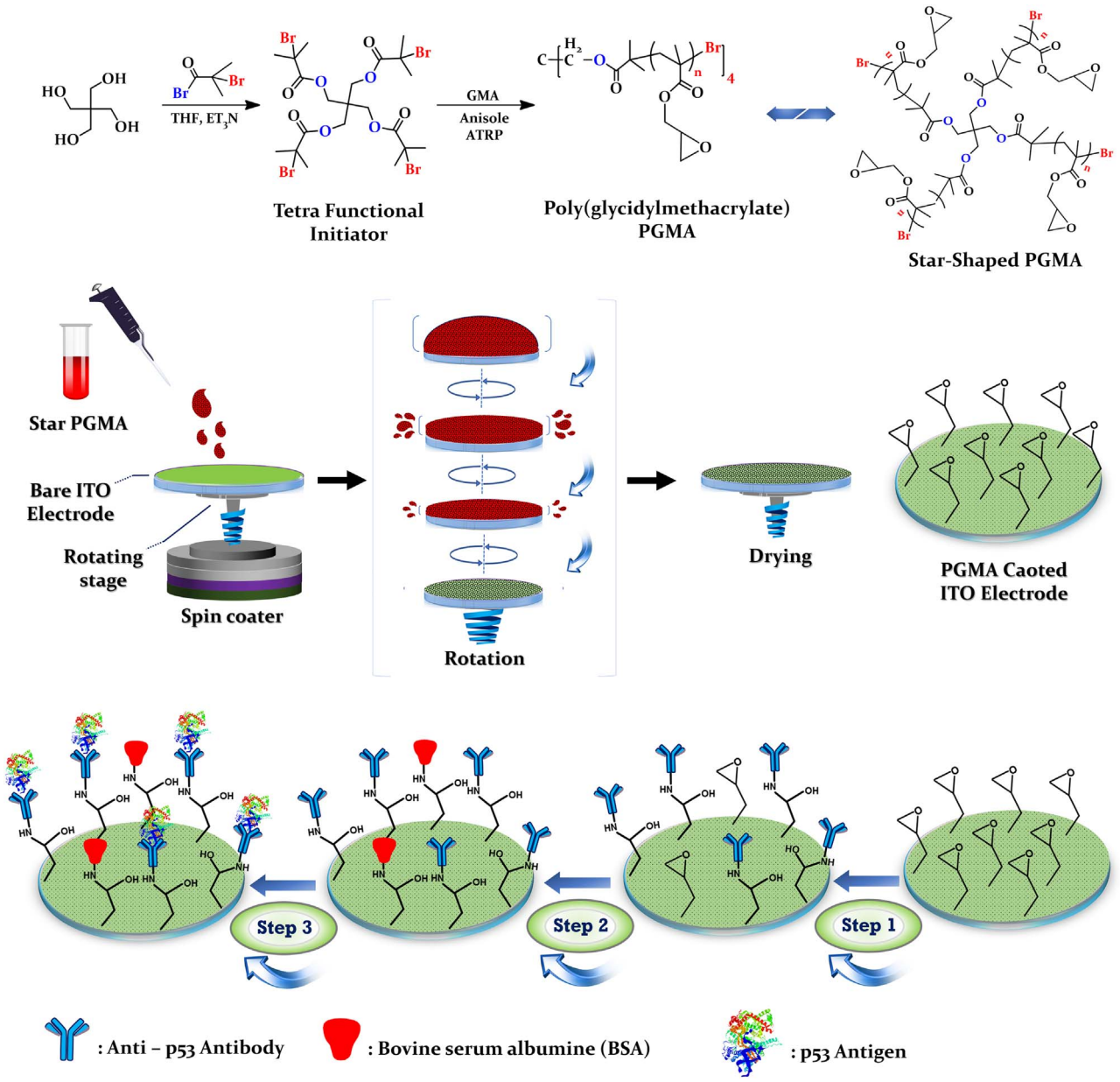


**Scheme 1.** Star-shaped $\mathbf{Star_{PGMA}}$ polymer synthesis and schematic illustration of the proposed electrochemical immunosensor.

applied potentials for cyclic voltammograms were between − 0.5 V and 1 V. EIS experiments were carried out in the frequency range from 0.5 to 50,000 Hz. The spin-coating process was performed using a traditional spin-coater (MTI VTC-50) at 1000 rpm for 60 s. The morphological characterization of the biosensor was performed with the help of Scanning Electron Microscope (SEM, FEI-Quanta FEG 250) and Atomic Force Microscope (AFM, NanoMagnetic Instruments, AFM PLUS+). Proton nuclear magnetic resonance ($^1$H NMR) spectra were obtained on a Bruker Avance III HD. Attenuated Total Reflection Fourier Transform Infrared (ATR-FTIR) measurements were carried out using a Bruker Company Vertex 70 FTIR infrared spectrometer in the range of 4000–400 $cm^{-1}$ at room temperature and the results were used without any corrections. Dispersive Raman measurements were performed with a Thermo company DXR Raman spectrometer equipped with a 780-nm excitation laser and a confocal microscope with 3 objectives. Average molecular weights and molecular weight distributions of the star-shaped polymer were estimated on an Agilent 1260 Infinity GPC/SEC instrument including a pump, refractive index detector, and two columns (Agilent PLgel 5 µm MIXED-C, 7.5 × 300 mm).

### 2.3. Synthesis of initiator and poly(glycidyl methacrylate) ($Star_{PGMA}$)

#### 2.3.1. Tetra functional initiator

The initiator was synthesized according to the literature method (Li et al., 2006; Yu et al., 2013). Pentaerythritol (1 g, 7.34 mmol) and triethylamine (88 mmol 12.2 mL) were added into a 100-mL round bottom flask containing 10 mL dry THF. The 10 mL THF solution of 2-bromoisobutyryl bromide (44 mmol, 5.44 mL) was added dropwise under Ar(g) atmosphere at 0 °C. Then, the reaction was stirred overnight at room temperature. The mixture was filtered and the solvent was removed by rotary evaporation. The remaining solid was dissolved in dichloromethane (DCM) and was washed with 50 mL 10% HCl (aq.) solution, 50 mL saturated $NaHCO_3$ (aq.) solution and water for two times, respectively. Finally, the organic layer was dried over anhydrous $MgSO_4$ and solvent removed by rotary evaporation. Pure product was obtained as a white solid by recrystallization from methanol. Yield 1.7 g (%32). FT-IR (ATR, $cm^{-1}$): 2982, 2935(-$CH_2$); 1733(C=O); 1473; 1390; 1372; 1270; 1160; 1100; 980; 935; 854; 762. Raman ($\lambda_{laser}$ = 780 nm): 2986, 2936 (-$CH_2$); 1738 (C=O); 1465; 1105; 1024; 1005; 918; 896;

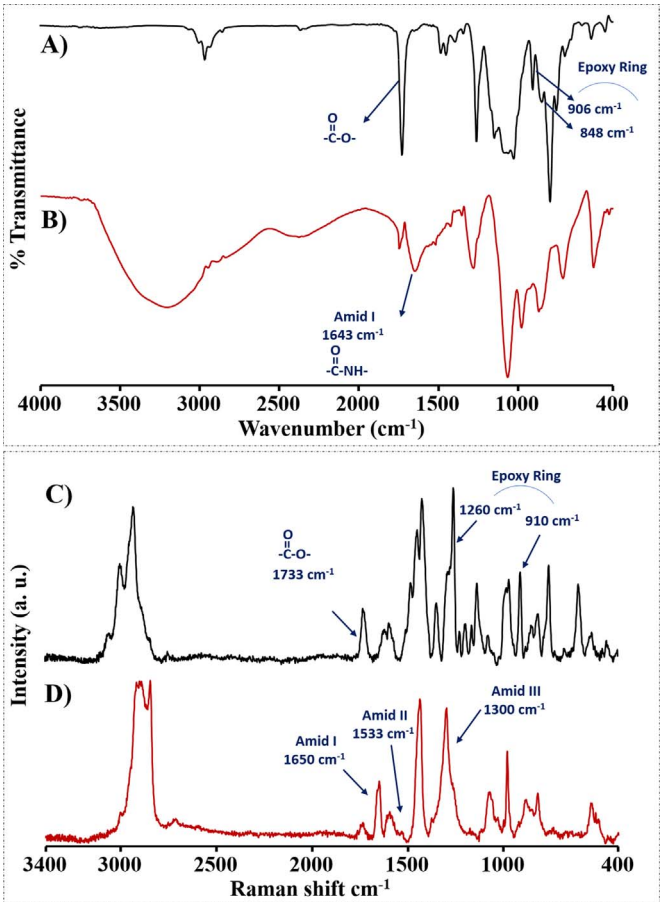


**Fig. 1.** FTIR and Raman spectra of **Star$_{PGMA}$** modified ITO electrode (A and B) and after anti-p53 immobilization on the ITO electrode (C and D). (For interpretation of the references to color in this figure, the reader is referred to the web version of this article.)

758; 644. $^{1}$H NMR ($CDCl_3$, 400 MHz) δ: 1,94 ppm (Ha; 24H), 4,33 ppm (Hb; 8 H). $^{13}$C NMR (100 MHz, $CDCl_3$, δ, ppm): 30.6 (a), 43.7 (e), 55.2 (b), 62.9 (d) and 170.1 (c). Mass spectrometer: $m/z$ = 732.8 [$M^{+1}$], $m/z$ = 731.8 (theoretical mass).

### 2.3.2. Star-shaped poly(glycidyl methacrylate)

The star-shaped poly(glycidyl methacrylate) was synthesized by an ATRP reaction between one equivalent of GMA monomer and 0.0025 equivalents of tetra functional initiator.(Aydin et al., 2016; Hayek et al., 2008) Tetra functional initiator (0.02 g, 0,0273 mmol), PMDETA (18.9 mg, 0.109 mmol), CuBr (15.6 mg, 0.109 mmol) and freshly distilled glycidyl methacrylate monomer (1.55 g, 10.9 mmol) were dissolved in 25 mL anisole, and the resulting solution was degassed by three freeze-pump-thaw cycle. The polymerization was carried out at 60 °C for 6 h. The polymerization was quenched by quickly cooling the tube in a water-ice bath and exposing the reaction mixture to air. Then, the green solution was filtered over neutral $Al_2O_3$ (eluent: $CH_2Cl_2$) to remove the copper-containing materials. The colorless filtrate was concentrated under reduced pressure; the residue was then dissolved in $CH_2Cl_2$ and precipitated twice in hexane, filtered and dried in vacuum at 30 °C overnight. Yield 1.27 (83%). $M_{n,\ NMR}$ = 26,887 g/mol $M_{n,\ GPC}$ = 31,320 g/mol; $M_{w,\ GPC}$ = 39,463, (Mw/Mn) PDI = 1,26. FTIR (ATR, cm−1): 3059, 3000, 2932 (-CH), 1725 (C=O), 1483; 1149; 1250; 1146; 992; 906; 845; 758; 695. Raman ($\lambda_{laser}$ = 780 nm): 3013; 2964, 2943; 1737 (C=O); 1460; 1267; 1145; 976; 916; 832; 770; 612. $^{1}$H NMR (400 MHz, $CDCl_3$, δ, ppm): 4.12 ppm(Ha), 1.89 ppm (Hb), 0.8–1.2 ppm (Hc), 3.8 ppm (Hd), 4.3 ppm (He), 3.23 ppm (Hf), 2.63 ppm (Hg), 2.83 ppm (Hh) ve 2.35 ppm (Hı).

### 2.4. Preparation of the Star$_{PGMA}$ modified ITO electrode

The preparation process of star-shaped **Star$_{PGMA}$** modified ITO electrodes includes three stages, as depicted in Scheme 1. First, thin bare ITO electrodes were cleaned by using ultrasonic bath in solutions of acetone, soap solution, and ultrapure water for 10 min each and dried under argon gas. Second, a solution of (**Star$_{PGMA}$**) in the appropriate ratio was spread over the entire surface of the ITO electrode. Finally, the spin-coater was accelerated to 1000 rpm rotational speed and maintained there for sixty seconds to evaporate the solvent.

### 2.5. Construction procedure of the electrochemical immunosensor

The immunosensor preparation process is schematically illustrated in Scheme 1. First of all, star-shaped **Star$_{PGMA}$** film was constructed by using spin-coating technique. Then, these electrodes were immersed into solution containing anti-p53 antibodies for 45 min, so they were immobilized onto ITO electrode via covalent bond formation. The free functional groups of star-shaped **Star$_{PGMA}$** were blocked by incubating electrodes in BSA solution for 1 h to prevent nonspecific interaction which could be formed between free ends and p53 antigen and other proteins. Afterwards, proposed biosensor got ready to measure p53 antigen.

### 2.6. Determination of p53 antigen

For the determination of p53 antigen, the prepared immunoelectrodes were immersed into PBS solution containing p53 antigen standard. After incubating 45 min in this solution, electrodes were washed ultra-pure water to remove non-interacted p53 antigens. To draw a calibration curve, 8 different concentrations of p53 were used. The relationship between the changes in impedance and concentrations of p53 was examined.

### 2.7. Real sample analysis

Serum samples were supplied by Namık Kemal University hospital. The serum samples were diluted 1000 times with PBS solution. To confirm the accuracy of the measurement technique, p53 standard solutions (0. 5 pg/mL) were added to these diluted samples. The determination of p53 in real samples was carried out by application of the procedures 2.6.

## 3. Results and discussions

### 3.1. Chemical characterization of initiator and polymer Star$_{PGMA}$

The tetra-armed star-shaped polymer with glycidyl side-groups were prepared using core-first approach (Scheme 1), which provided good control on the macromolecular architecture (Wycisk et al., 2015). The chemical structure of initiator and **Star$_{PGMA}$** were characterized by different spectral techniques (FTIR and $^{1}$H NMR, $^{13}$C NMR, RAMAN and MASS spectroscopy) to show the success of the synthesis method of the chemical compounds and results were displayed in detail in the Supplementary information file.

The FTIR spectra of polymer **Star$_{PGMA}$** modified ITO electrode surface before anti-p53 immobilization (black line) and after anti-p53 immobilization (red line) are shown in Figs. 1A and 1B, respectively. As seen in Fig. 1A, the star polymer modified ITO surface had the two absorption peaks at 906 $cm^{-1}$ and 848 $cm^{-1}$ that indicated the presence of epoxy group in **Star$_{PGMA}$** (Oh et al., 2010). The strong signal observed around 1725 $cm^{-1}$ was attributed to C=O stretching vibration of carbonyl groups (Aydın et al., 2011). At red line in Fig. 1B, there were broad and intense bands for amide I at ~ 1645 $cm^{-1}$ and for amide II at ~ 1523 $cm^{-1}$, and this clearly illustrated the presence of the anti-p53 antigen compound and immobilization of anti-p53 to polymer

**Star$_{PGMA}$** modified ITO electrode surface (Banas et al., 2015). The chemical structures of **Star$_{PGMA}$** modified ITO electrode and anti-p53 antibody immobilized ITO electrode were also examined via Raman spectroscopy (Figs. 1C and 1D). The chemical structure of polymer and the molecular structure of proteins are usually investigated by using Raman spectroscopy (Austin et al., 2016; Chen and Lord, 1974; Kurouski et al., 2015). The Raman spectra showed that epoxy ring stretching vibrations of **Star$_{PGMA}$** were observed at 1260 $cm^{-1}$ and 910 $cm^{-1}$. Raman spectral technique has been proved to be a convenient tool to identify amide bonds. Amide I, II and III regions are monitored mostly between 1650 and 1680 $cm^{-1}$, 1480–1570 $cm^{-1}$ and 1235–1300 $cm^{-1}$, respectively (Kitagawa and Hirota, 2002). As shown in Fig. 1D, amide I, amide II and amide III bonds were observed at 1650, 1533 and 1300 $cm^{-1}$, respectively (Rygula et al., 2013).

### 3.2. Electrochemical characterization of p53 immunosensor

In the present work, a star-shaped polymer film was constructed on the ITO electrode by using a spin coating technique. The polymer **Star$_{PGMA}$** provided a lot of epoxy groups for binding of amino groups of antibodies. This step is important to develop a sensitive biosensor construction. Electrochemical behaviors of each modification step of the immunosensor were monitored by EIS and cyclic voltammograms (CV). The EIS spectra and the CV voltammograms of the fabricated biosensor are illustrated in Fig. 2.

EIS is widely used to validate the layer-by-layer deposition of materials onto a sensor surface because it is a very powerful tool for surface interface characterization and detection of changes formed onto biosensor surfaces (Wang et al., 2017b). Here, impedance measurements were carried out at each stage of the assembly. The EIS spectra were analyzed using Gamry Echem Analyst software. The Nyquist plot is composed of two parts: the semicircle part at higher frequencies belonging to the electron-transfer limited process and the linear portion at lower frequency range regards to the diffusion-limited process. The diameter of the semicircle is defined as the change transfer resistance ($R_{ct}$) (Cho et al., 2012). The interfacial charge-transfer resistance ($R_{ct}$) changed after each layer formation, namely polymer **Star$_{PGMA}$**, anti-p53 antibody, BSA and p53 antigen and these variations are illustrated in Fig. 2A. This indicated the successful construction of the immunosensor. It is widely reported that analyte binding to biosensor surfaces often causes increased impedance, typically due to increasing deposition of a substance on the sensor surface which increases its surface capacitance and resistance. General EIS parameters are $R_s$ (solution resistance), $R_{ct}$ (charge-transfer resistance) and $C_p$ (constant phase element, an equivalent model of double-layer capacitance) (Bahadır and Sezgintürk, 2016a). The signal of the biosensor was calculated by fitting the data to the Randles′ equivalent circuit (Fig. 1 inset). The polymer **Star$_{PGMA}$** modified ITO had a large semicircle diameter due to the introduction of polymer film including epoxy groups. After immobilization of anti-p53 antibodies on the polymer modified ITO, the $R_{ct}$ decreased significantly. After blockage of free epoxy ends with BSA, an increase was observed in $R_{ct}$ value. After interaction between anti-p53 antibody and p53 antigen, the $R_{ct}$ value was increased due to increment in insulating property. Consequently, a sensitive and selective immunosensor was successfully fabricated with the association of sensitive EIS change and specific immunoreaction between anti-p53 antibody and p53 antigen.

Cyclic voltammetry measurement was performed to evaluate the variations formed on the electrode surface via monitoring electrochemical activity of the redox couple at all of the immobilization steps. As seen figure in 2B, a pair of reversible redox peaks were obtained after **Star$_{PGMA}$** was coated onto the ITO electrode. The antibody loading on the ITO electrode increased the peak currents. After blocking of free active epoxy ends, the peak currents were decreased because the amount of bounded proteins were increased. After interaction between anti-p53 antibody and p53 antigen, a decrease was observed at redox peak currents owing to the insulating property of the proteins. This result proved the successful loading of the biomolecules on the ITO electrode surface.

### 3.3. Morphological characterization of p53 immunosensor

In this study, SEM and AFM were used to characterize the morphology and composition of the **Star$_{PGMA}$** based immunosensor. Fig. 3 depicts the SEM and AFM images of the ITO electrode in different immobilization steps. The surface roughness of the unmodified ITO electrode is clearly as seen in Fig. 3A. The root mean square (RMS) value was very low (3.06 nm). The bare ITO surface had a smooth and homogenous surface (Fig. 3B). The AFM images of **Star$_{PGMA}$** film illustrated a homogenous surface with good dispersion (Fig. 3C). Visibly, a dense **Star$_{PGMA}$** layer was obtained completely on the ITO surface to construct the surface area for immobilization of biorecognition element (Fig. 3D). After anti-p53 antibody immobilization, the AFM images indicated the obvious morphological change. Also, after loading anti-p53 antibodies, the clear images were seen, indicating that **Star$_{PGMA}$** can be used as a good matrix for anti-p53 antibodies. **Star$_{PGMA}$** polymer acted as a polymer backbone to give a stable and homogenous film (Fig. 3E). In SEM image, after coupling of anti-p53 antibodies on the ITO electrode surface, it can be seen that an apparent layer was formed on the modified ITO electrode (Fig. 3F). Additionally, BSA was used to blockage the active epoxy ends. As seen in Figs. 3G and 3H, BSA was coated on the ITO surface. After specific interaction antibody and antigen, the morphological image was changed (Figs. 3I and 3J). The RMS values were found as 29.92, 104.32, 41.21, and 52.81 nm after anti-p53 antibody, BSA and p53 antigen immobilization, respectively. Also, these images clearly confirmed the biosensor construction steps. After investigation of SEM and AFM pictures, it can be concluded that the results are in intercompatibility.

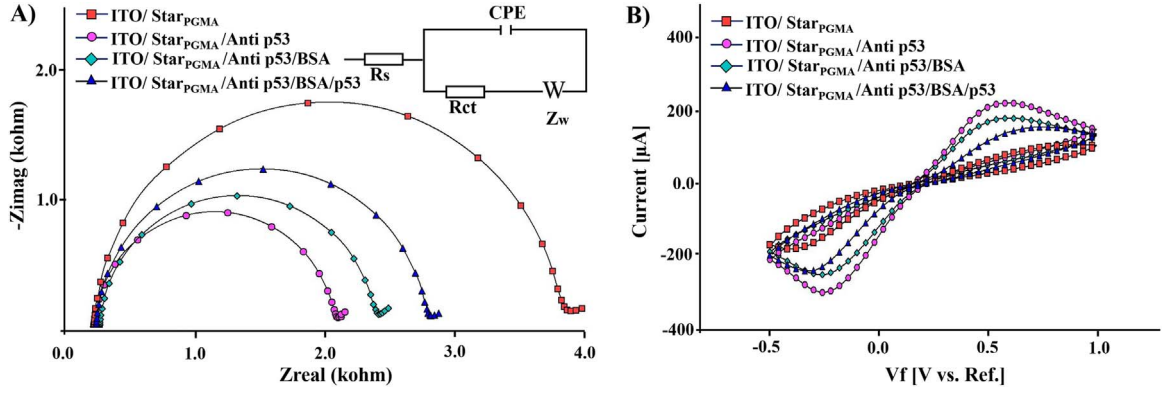


**Fig. 2.** Impedance spectra (A) and cyclic voltammograms of the proposed immunosensor during the fabrication steps.

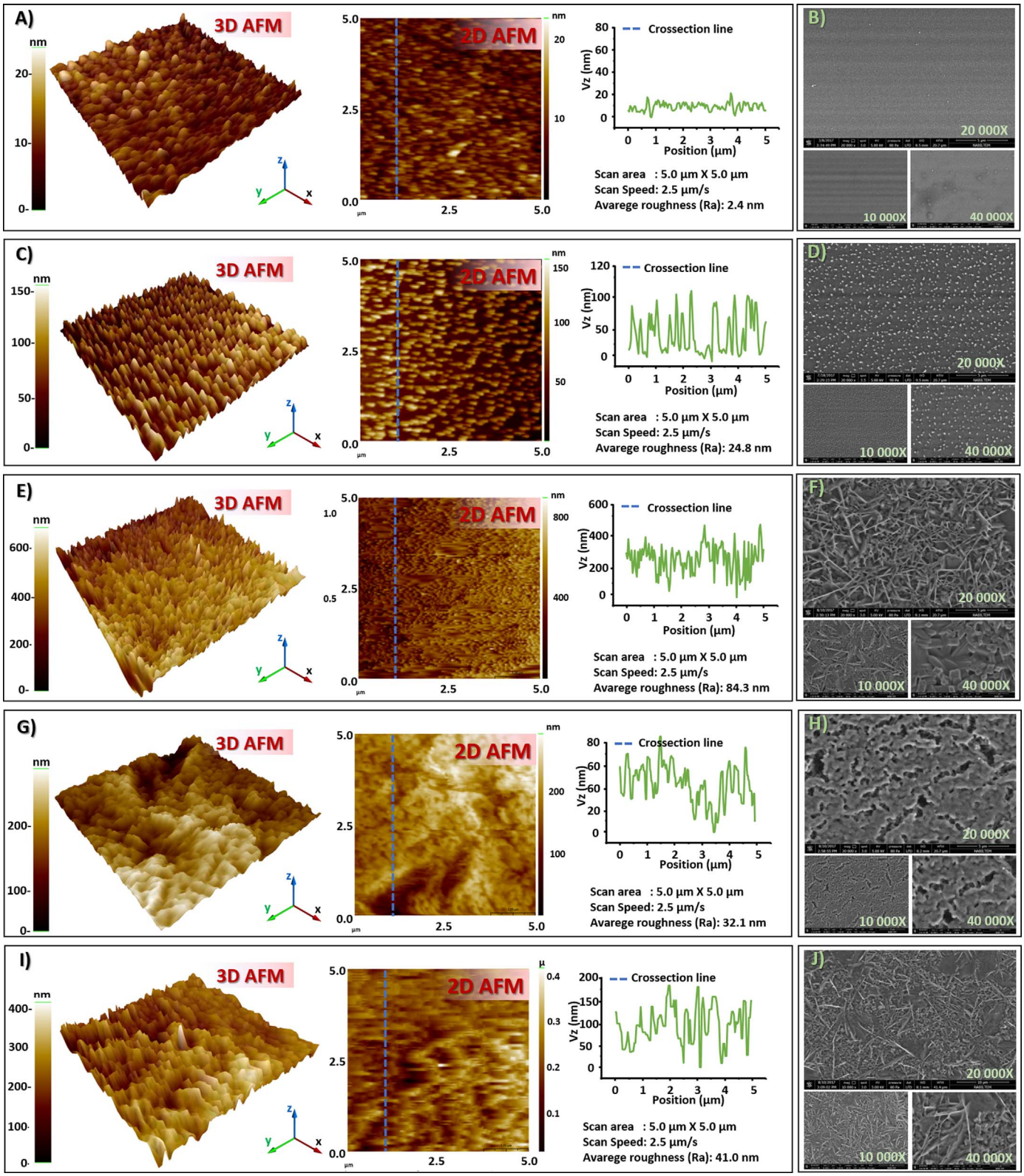


**Fig. 3.** SEM and AFM images of bare ITO electrode (A, B), **Star$_{PGMA}$** modified ITO electrode (C, D), after anti-p53 immobilization (E, F), BSA blockage (G, H), after specific interaction between anti-p53 antibody and p53 antigen (I and J).

### *3.4. Optimization studies in biosensor preparation*

To obtain high sensitivity for p53 antigen detection, the experimental conditions were optimized in terms of polymer concentration, antibody concentration, antibody and antigen incubation time experiments.

Different **Star$_{PGMA}$** polymer solutions (0.1%, 0.25%, and 0.5%) were prepared by using acetone due to its fast evaporation property during spin coating process. With the increase of polymer **Star$_{PGMA}$** concentration, a lot of epoxy groups were formed on the ITO electrode

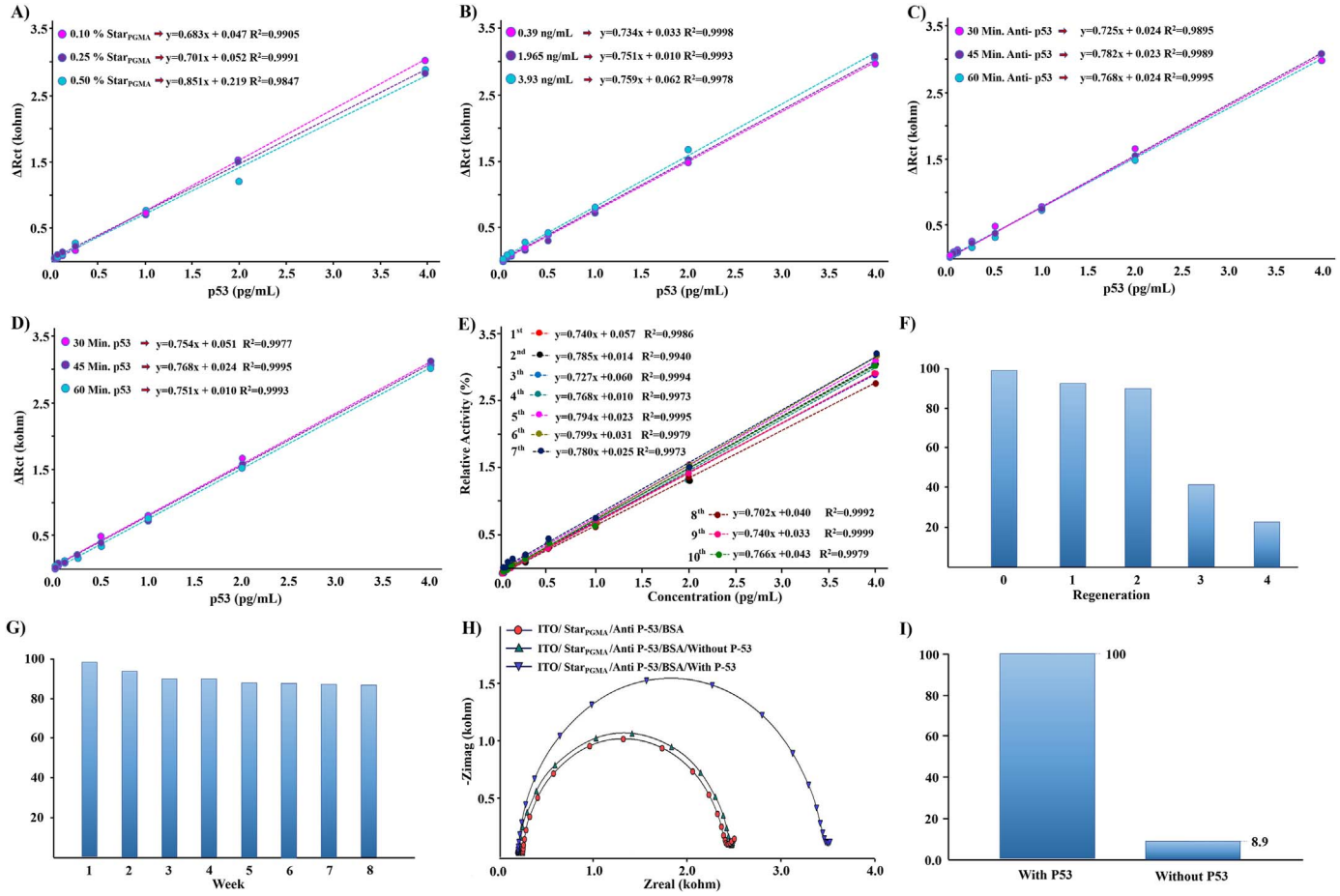


**Fig. 4.** Optimization results of **Star$_{PGMA}$** polymer concentration (A), anti-p53 antibody concentration (B), anti-p53 antibody incubation time (C), p53 antigen incubation time (D); results of reproducibility (E), regeneration (F), stability (G), interference (H and I) studies.

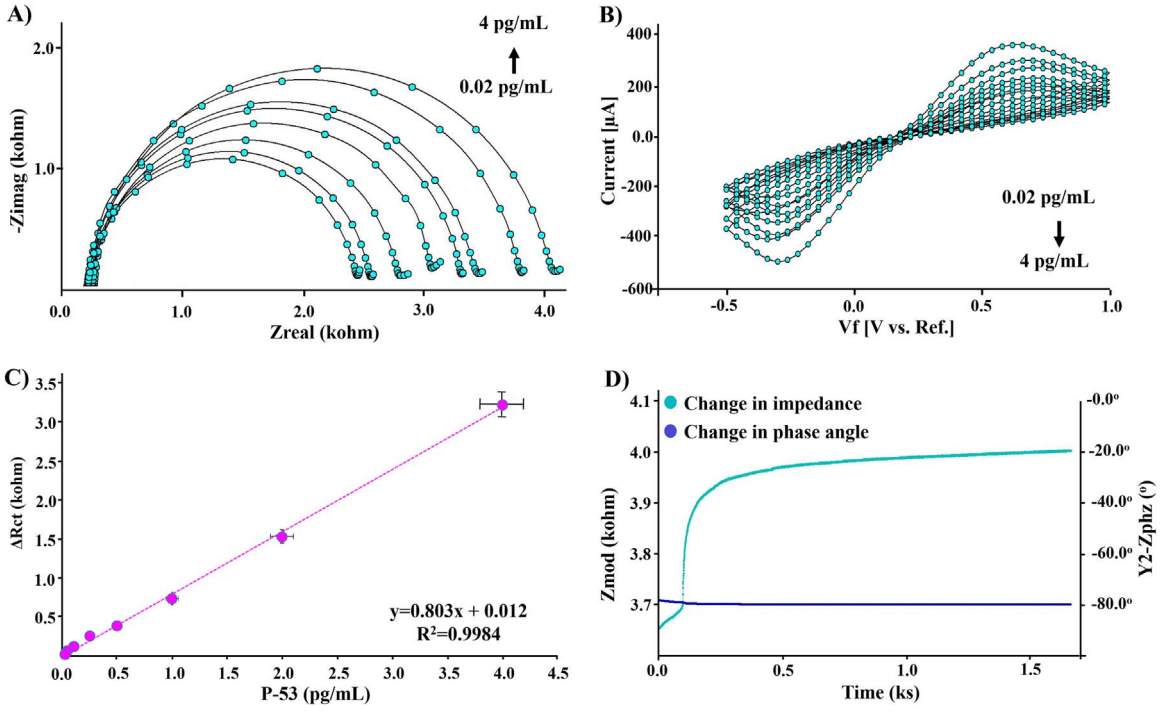


**Fig. 5.** Nyquist plots of impedance spectra and cyclic voltammograms of the proposed immunosensor after incubation with different concentrations of p53 (A and B), Calibration curve of p53 (C), SFI spectra of after specific interaction between p53 antibody and p53 antigen (D).

surface and the conductivity of ITO electrode was decreased and therefore low signals were obtained. Therefore, 0.1% polymer concentration was chosen as optimum value (Fig. 4A). During the biosensor fabrication, three different amounts (0.39 ng/mL, 1.965 ng/mL and 3.93 ng/mL) of anti-p53 antibodies were utilized. When 0.39 ng/mL antibody concentration was utilized, a bit low signal than the other concentrations was measured. The signals were similar when 1.965 ng/mL and 3.93 ng/mL antibody concentrations were utilized. Therefore, 1.965 ng/mL antibody concentration was chosen as optimum value (Fig. 4B). The biorecognition element immobilization is important and this process was affected from incubation time of antibodies. Therefore, three different incubation periods (30 min, 45 min and 60 min) were examined and the highest signal was obtained at 45 min (Fig. 4C). Thus, 45 min incubation time was selected for the following studies. Apart from antibody incubation time, antigen incubating time was also studied. As shown in Fig. 4D, different incubation times of antigen from 30 min to 60 min were investigated, and 45 min was selected as the optimum incubation duration. Statistical analyses were performed by using PASW Statistic 18 program. The test method was One Sample T Test and this test performed in 95% confidence interval. The statistical test showed that concentration optimization studies (polymer and antibody concentration optimization) results had no statistical meaningful because $p = 0.117$ value found with T test were higher than 0.05. And incubation time optimization studies (antibody and antigen concentration optimization) results had statistically meaningful because $p = 0.035$ value found with T test were lower than 0.05.

### 3.5. Analytical performance of electrochemical immunosensor

In order to determine the performance of the immunosensor, the prepared electrochemical immunosensor was used to determine different concentrations of p53 under optimal sensing conditions. Figs. 5A and 5B show the impedance spectra and cyclic voltammograms of the proposed immunosensor incubated in increased concentration of p53, respectively. As seen in impedance spectra, upon increasing concentration of p53, we observed an increment in $R_{ct}$ value, because the increasing numbers of p53 antigen covered the ITO electrode surface thus a more insulative layer was formed on the ITO electrode (Fig. 5A). On the contrary to $R_{ct}$ values, peak currents were decreased in cyclic voltammograms. Because the formed insulative layer prevented the redox probe influence from the electrolyte solution to electrode surface (Fig. 5B).

To determine a calibration curve for p53 antigen, the impedimetric responses were recorded and the charge transfer resistance ($R_{ct}$) values were calculated based on best fit of the equivalent circuit model including solution resistance ($R_s$), charge transfer resistance ($R_{ct}$), Warburg resistance (W) and constant phase element (CPl). A linear relationship was monitored between the impedimetric signal and the p53 concentrations over a range of 0.02–4 pg/mL with a correlation coefficient of 0.998 (Fig. 5C). The limit of detection (LOD; 3 fold of blank sample signal/slope) and limit of quantification (LOQ; 10 fold of blank sample signal/slope) were calculated as 7 fg/mL and 22 fg/mL, respectively. The main analytical parameters and performances of the developed p53 biosensors are compared and are summarized in SI-Table 1. The proposed immunosensor had a low detection limit compared to the previously reported biosensors due to a lot of epoxy groups of $\mathbf{Star_{PGMA}}$. Furthermore, the proposed immunosensor displayed a large surface area to immobilize a lot of biorecognition elements and to achieve a wide linear range.

To monitor specific interaction between anti-p53 antibodies and p53 antigens, SFI technique was utilized. The principle of this technique was based on impedance measurement at constant frequency value (van Duuren et al., 2017). To determine the frequency, Bode plot was utilized. During constant frequency value, an increase was observed in impedance (pink). This increase was a sign of specific interaction (Fig. 5D).

The repeatability of the immunosensor was tested by using twenty electrodes to detect the same concentration of p53 (0.50 pg/mL) under identical conditions. The relative standard deviation (RSD) was calculated to be 5.74%. The proposed biosensor was successfully used for the accurate determination of p53 antigen and the results indicated good repeatability for p53. The reproducibility of the immunosensor was examined by preparing ten different immunosensor series including at least equally prepared 80 electrodes. The relative standard deviation (RSD) was calculated to be 4.15% and this indicated the good reproducibility of the fabricated immunosensor (Fig. 5E).

Reusability is an important parameter to decrease the analysis cost. The possibility of reusing the biosensor for several times through a regeneration step was explored. To investigate the reusability of the immunosensor, the immunosensor was exposed to acidic solution (ultra-pure water; HCl, 0.1%) for 5 min. Firstly, the standard solution including p53 was measured by using the prepared biosensor, then it immersed in acidic solution to break specific interaction between antigen and antibody. After that, the standard solution including p53 was re-measured by using the regenerated biosensor. After each regeneration step the $R_{ct}$ value was decreased due to denaturation of p53 antibodies on the modified ITO electrode. Our proposed immunosensor illustrated 22.40% activity after four cycles (Fig. 5F). Also, our immunosensor was suitable for reutilization.

The storage stability of the fabricated biosensors was investigated through measuring the EIS signals of ten electrodes prepared independently every week. The electrodes were kept in dry form at + 4 °C. The obtained EIS signals maintained about 87.8% of its original values after eight weeks, indicating acceptable stability (Fig. 5G).

The selectivity of the fabricated immunosensor was evaluated for the determination of 0.5 ng/mL p53 antigen together with various interferences, including biomarkers (Vascular Endothelial Growth Factor (VEGF), Receptor for Activated C Kinase (RACK1), Tumor necrosis factor α (TNF α), Interleukin 8 (IL-8)), drugs (ampicillin, amoxycillin, aspirin) at a relatively high concentration (100 ng/mL). Evidently only p53 showed a considerable change in $\Delta R_{ct}$ value. Also, no substantial signals of other biomarkers and drugs were observed, further confirming the excellent selectivity of the proposed immunosensor (Fig. 5H-I).

To investigate the feasibility of the developed immunosensor, human serum samples were used as real samples after 1000 fold dilution. The chemical composition of human serum is complex, containing proteins, ions, nutrients and other substances (Yoshida et al., 2017). Some of these components could interfere with the detection signal, causing an unspecific $R_{ct}$. The recovery experiments were carried out by adding standard p53 antigen solutions to the healthy human serum samples and the recoveries were ranging from 94.0% to 104.4% (SI-Table 1). This result demonstrated that the immunosensor can be utilized to determine p53 in human serum samples.

## 4. Conclusion

Here, for the first time, an electrochemical immunosensor was developed for p53 antigen detection using a disposable spin-coated ITO electrode. By using spin-coating technique, a homogenous film was formed on the ITO electrode surface and this film was efficient for covalent binding of anti-p53 antibodies. The most important advantages of spin coating technique were the easiness, low-cost and practicality of this method. The modified ITO electrodes were prepared with high speed. The CV and EIS techniques were utilized to follow the individual steps of modified electrode fabrication and antibody-antigen interaction at the electrode surface. The antibody coupling on the electrode surface was proved by FTIR and Raman spectral techniques. Furthermore, morphological characterization was performed by using SEM and AFM. A linear relationship between the electron-transfer resistance and the p53 antigen concentration was found in the range of 0.02–4 ng/mL. The fabricated immunosensor illustrated a high

reproducibility (4.15%) and sensitivity (7 fg/mL) for p53 antigens measurements. Furthermore, the results of real samples analysis showed that this system was an alternative approach to p53 antigen analysis in clinical routine.

## Acknowledgement

This research was supported by The Scientific and Technological Research Council of by Namık Kemal University, NKU-BAP (Grant number: NKUBAP.00.DS.17.114).

## Appendix A. Supplementary material

Supplementary data associated with this article can be found in the online version at http://dx.doi.org/10.1016/j.bios.2018.02.017.

## References

Afsharan, H., Khalilzadeh, B., Tajalli, H., Mollabashi, M., Navaeipour, F., Rashidi, M.-R., 2016a. Electrochim. Acta 188, 153–164.
Afsharan, H., Navaeipour, F., Khalilzadeh, B., Tajalli, H., Mollabashi, M., Ahar, M.J., Rashidi, M.-R., 2016b. Biosens. Bioelectron. 80, 146–153.
Attallah, A.M., Abdel-Aziz, M.M., El-Sayed, A.M., Tabll, A.A., 2003. Cancer Detect. Prev. 27 (2), 127–131.
Austin, L.A., Osseiran, S., Evans, C.L., 2016. Analyst 141 (2), 476–503.
Aydın, E.B., Aydın, M., Sezgintürk, M.K., 2017. Biosens. Bioelectron. 97, 169–176.
Aydın, E.B., Sezgintürk, M.K., 2017. Talanta 172, 162–170.
Aydın, M., Esat, B., Kılıç, Ç., Köse, M., Ata, A., Yılmaz, F., 2011. Eur. Polym. J. 47 (12), 2283–2294.
Aydin, M., Gorur, M., Yilmaz, F., 2016. React. Funct. Polym. 102, 11–19.
Bahadır, E., Sezgintürk, M., 2016a. Analyst 141 (19), 5618–5626.
Bahadır, E.B., Sezgintürk, M.K., 2015. Talanta 132, 162–174.
Bahadır, E.B., Sezgintürk, M.K., 2016a. Talanta 148, 427–438.
Bahadır, E.B., Sezgintürk, M.K., 2016b. Artif. Cells Nanomed. Biotechnol. 44 (1), 248–262.
Banas, A., Banas, K., Furgal-Borzych, A., Kwiatek, W., Pawlicki, B., Breese, M., 2015. Analyst 140 (7), 2156–2163.
Ben-Hur, H., Berman, V., Sandler, B., Smirnoff, P., Gurevich, P., Zusman, I., 1997. Eur. J. Gynaecol. Oncol. 18 (5), 400–406.
Bryś, M., Semczuk, A., Wójcik, M., Krajewska, W.M., Jakowicki, J.A., 2000. Cancer Lett. 148 (2), 197–205.
Chen, A., Bao, Y., Ge, X., Shin, Y., Du, D., Lin, Y., 2012. RSC Adv. 2 (29), 11029–11034.
Chen, M., Lord, R., 1974. J. Am. Chem. Soc. 96 (15), 4750–4752.
Cho, M., Chun, L., Lin, M., Choe, W., Nam, J., Lee, Y., 2012. Sens. Actuators B 174, 490–494.
El-Said, W.A., Choi, J.-W., 2014. Electrochim. Acta 123, 51–57.
Feng, Q., Yu, M., Kiviat, N.B., 2006. Crit. Rev. Clin. Lab. Sci. 43 (5–6), 497–560.
Fung, K.Y., Tabor, B., Buckley, M.J., Priebe, I.K., Purins, L., Pompeia, C., Brierley, G.V., Lockett, T., Gibbs, P., Tie, J., 2015. PLoS One 10 (3), e0120425.
Gao, H., Matyjaszewski, K., 2009. Prog. Polym. Sci. 34 (4), 317–350.
Hayek, A., Xu, Y., Okada, T., Barlow, S., Zhu, X., Moon, J.H., Marder, S.R., Yang, S., 2008. J. Mater. Chem. 18 (28), 3316–3318.
Inoue, K., 2000. Prog. Polym. Sci. 25 (4), 453–571.
Jeon, N.J., Noh, J.H., Kim, Y.C., Yang, W.S., Ryu, S., Seok, S.I., 2014. Nat. Mater. 13 (9), 897–903.
Karimi-Maleh, H., Biparva, P., Hatami, M., 2013. Biosens. Bioelectron. 48, 270–275.
Kitagawa, T., Hirota, S., 2002. Raman Spectroscopy of Proteins. Handbook of Vibrational Spectroscopy.
Kurouski, D., Van Duyne, R.P., Lednev, I.K., 2015. Analyst 140 (15), 4967–4980.
Li, J., Shi, L., An, Y., Li, Y., Chen, X., Dong, H., 2006. Polymer 47 (26), 8480–8487.
Makelane, H.R., Tovide, O., Sunday, C.E., Waryo, T., Iwuoha, E.I., 2015. Sensors 15 (9), 22343–22363.
Marley, A.R., Nan, H., 2016. Int. J. Mol. Epidemol. Genet. 7 (3), 105.
Norrman, K., Ghanbari-Siahkali, A., Larsen, N., 2005. Annu. Rep. Prog. Chem. Sect. C: Phys. Chem. 101, 174–201.
Oh, J., Lee, J.-H., Koo, J.C., Choi, H.R., Lee, Y., Kim, T., Luong, N.D., Nam, J.-D., 2010. J. Mater. Chem. 20 (41), 9200–9204.
Ruecha, N., Rangkupan, R., Rodthongkum, N., Chailapakul, O., 2014. Biosens. Bioelectron. 52, 13–19.
Rygula, A., Majzner, K., Marzec, K.M., Kaczor, A., Pilarczyk, M., Baranska, M., 2013. J. Raman Spectrosc. 44 (8), 1061–1076.
Satija, J., Sai, V., Mukherji, S., 2011. Dendrimers in biosensors: concept and applications. J. Mater. Chem. 21 (38), 14367–14386.
Singh, A., Choudhary, M., Kaur, S., Singh, S.P., Arora, K., 2016. Mater. Today: Proc. 3 (2), 157–161.
Soylemez, S., Udum, Y.A., Kesik, M., Hızlıateş, C.G., Ergun, Y., Toppare, L., 2015. Sens. Actuators B 212, 425–433.
Topkaya, S.N., Azimzadeh, M., Ozsoz, M., 2016. Electroanalysis 28 (7), 1402–1419.
Turner, A.P., 2013. Biosensors: sense and sensibility. Chem. Soc. Rev. 42 (8), 3184–3196.
Tyona, M., 2013. A theoritical study on spin coating technique. Adv. Mater. Res. 2 (4), 195–208.
van Duuren, J.B., Müsken, M., Karge, B., Tomasch, J., Wittmann, C., Häussler, S., Brönstrup, M., 2017. Sci. Rep. 7.
Wang, B., Akiba, U., Anzai, J.-I., 2017a. Molecules 22 (7), 1048.
Wang, S.X., Acha, D., Shah, A.J., Hills, F., Roitt, I., Demosthenous, A., Bayford, R.H., 2017b. Biosens. Bioelectron. 92, 482–488.
Wang, X., Gao, C., Shu, G., Wang, Y., Liu, X., 2015. J. Electroanal. Chem. 756, 101–107.
Wycisk, A., Döring, A., Schneider, M., Schönhoff, M., Kuckling, D., 2015. Polymers 7 (5), 921.
Xu, M., Luo, X., Davis, J.J., 2013. Biosens. Bioelectron. 39 (1), 21–25.
Yoshida, T., Lee, S.Y., Nielsen, J., Stephanopoulos, G., 2017. John Wiley & Sons.
Yu, Z.-Q., Lam, J.W., Zhao, K., Zhu, C.-Z., Yang, S., Lin, J.-S., Li, B.S., Liu, J.-H., Chen, E.-Q., Tang, B.Z., 2013. Polym. Chem. 4 (4), 996–1005.
Zusman, I., 1998. J. Chromatogr. B: Biomed. Sci. Appl. 715 (1), 297–306.